Supporting Information

Phosphorus-doped $CoTe_2$/C nanoparticles create new Co-P active sites to promote hydrogen evolution reaction

Qingtao Wang,*[a] Kai Cui,[a] Jian Li,[a] Yanxia Wu,[a] Yaoxia Yang,[a] Xiaozhong Zhou,[a] Guofu Ma,[a] Zhiwang Yang,[a] Ziqiang Lei,[a] Shufang Ren*[b]

a Key Laboratory of Eco-functional Polymer Materials of the Ministry of Education, Key Laboratory of Eco-environmental Polymer Materials of Gansu Province, College of Chemistry and Chemical Engineering, Northwest Normal University, Lanzhou 730070, China E-mail: wangqt@nwnu.edu.cn

b Key Laboratory of Evidence Science Research and Application of Gansu Province, Gansu University of Political Science and Law, Lanzhou 730070, China E-mail: rsf@gsli.edu.cn

Material Characterization.

The crystal structures of the products were determined by powder X-ray diffraction (XRD, X'Pert PRO, Netherlands). The structures and morphologies were sequentially assessed using field-emission transmission electron microscopy (TEM, FEI TECNAI G^2 TF20, America) and scanning electron microscopy (FESEM, Carl Zeiss Ultra plus, Germany). X-ray photoelectron spectroscopy (XPS) was collected on a PHI-5702 multifunctional photoelectron spectromete (America) equipped with monochromated Al K alpha.

Electrochemical Characterization.

All electrochemical tests were carried out an Autolab PGSTAT128N (Switzerland) electrochemical workstation using a standard three-electrode glass cell. A glassy carbon electrode with a diameter of 5 mm was used as the working electrode, Ag/AgCl immersed in a saturated KCl solution as the reference electrode, and graphite rod as the counter electrode. Convert all measured potentials to a reversible hydrogen electrode (RHE) potential by the Nernst equation: E (RHE) = E (Ag/AgCl) +0.059 pH+0.197. An aqueous solution of 0.5 M H_2SO_4 and 1.0 M KOH were used as the electrolyte. In order to eliminate the interference of O_2 before each electrochemical measurement, the electrolyte was bubbled with N_2 for 30 minutes. The working electrode was manufactured as follows: 5 mg of P-$CoTe_2$/C nanoparticle catalysts were dispersed in a mixture solution of 480 μL ethanol, 500 μL water, and 20 μL Nafion solution (5 wt.%). The mixture was sonicated for 30 min to form uniformly catalyst ink. Then, 10 μL of the catalyst ink was dropped on a 5 mm diameter glassy carbon electrode, and dried at room temperature to obtain a working electrode (catalyst loading ~0.2 mg cm^{-2}). The polarization curves were corrected by iR compensation (80%) to eliminate the interference of the ohmic resistance. The double layer capacitance (C_{dl}) was determined by cyclic voltammetry (CV) scanning at different scan rates from 30 mV s^{-1} to 150 mV s^{-1}. The electrochemical impedance spectroscopy (EIS) measurement was performed at the corresponding open circuit potential of the electrode in the frequency range of 50 kHz to 0.01 Hz, and the resistance of the solution was determined by the obtained Nyquist diagram.

TOF calculation:

The turnover frequency (TOF, s^{-1}) for HER was calculated with the following equation:

$$TOF=(|J|\times A)/2Fn \quad (1)$$

Where $|J|$ ($A\cdot cm^{-2}$) is the current density at a fixed voltage during the LSV measurement, A is the geometric area of the working glassy carbon electrode (0.19625 cm^2), the factor of 2 is the corresponding electron transfer numbers, F is the Faraday constant (96485 $C\cdot mol^{-1}$), and n is the number of active sites (mol).

$$n=Q/2F=It/2F=IV/v2F=S/v2F \quad (2)$$

The number of active sites (n) was determined by the cyclic voltammetry (CV) in pH = 7 phosphate buffer with a scan rate of 50 mV s^{-1}. The number of the voltammetric charges (Q) could be determined by integrating. Where I is the current (A), V is the voltage (mV), v is the scan rate (50 $mV\cdot s^{-1}$), S is integrated effective area in CV plot.

Computational Details

Density functional theory (DFT) calculations were performed using the Perdew-Burke-Ernzerzerbof (PRE) form of generalized gradient approximation functional (GGA) by employing Vienna ab-initio simulation package (VASP)[1, 2]. The energy cutoff of plane wave was set as 400 eV[3]. and the Monkhorst-Pack grid was built as 3×3×1 k-point mesh though out the calculations[4]. The energy and force were converged to 1.0×10^{-6} eV $atom^{-1}$ and 0.01 eV $Å^{-1}$, respectively. The spin polarization was considered in all calculation. The Fermi scheme was employed for electron occupancy with an energy smearing of 0.1 eV.

Model

The $CoTe_2$ (111) surface was obtained by cutting the $CoTe_2$ bulk along the direction. In all structural optimization calculations, the bottom atoms were fixed, while the other atoms were allowed to relax. A vacuum layer as large as 15 Å was used along the c direction normal to the surface to avoid periodic interactions. For the P doing, one surface Te atom of $CoTe_2$ was replaced by P atom.

For hydrogen evolution reaction, the Gibbs free-energy change of the H was employed to estimate the activity of the catalyst. The Gibbs free-energy change

(ΔG_{ads}) of H was defined as follows

$$G_{ads} = E_{ads} + E_{ZPE} - TS \qquad (Eq.1)$$

Where E_{ads} was the adsorption energy of the atomic H on the $CoTe_2$ (111) surface, E_{ZPE} was the difference in zero-point energy between the adsorbed hydrogen and hydrogen in the gas phase. ΔS was the entropy change of one H atom from the absorbed state to the gas phase. The first two terms were calculated with the same parameters. The third term was calculated by setting the isolated H_2 in a box of 12 Å ×12 Å × 12 Å.

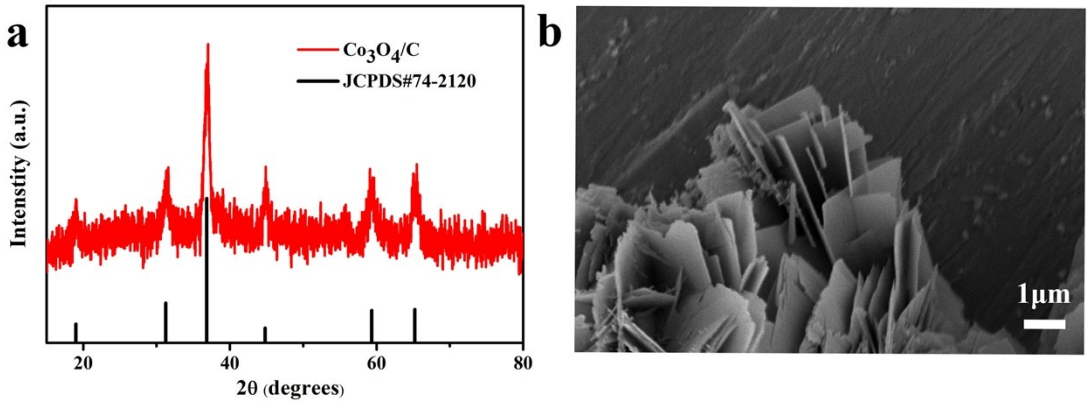

Fig. S1 (a) XRD pattern of Co_3O_4/C nanosheets. (b) SEM image of Co_3O_4/C nanosheets.

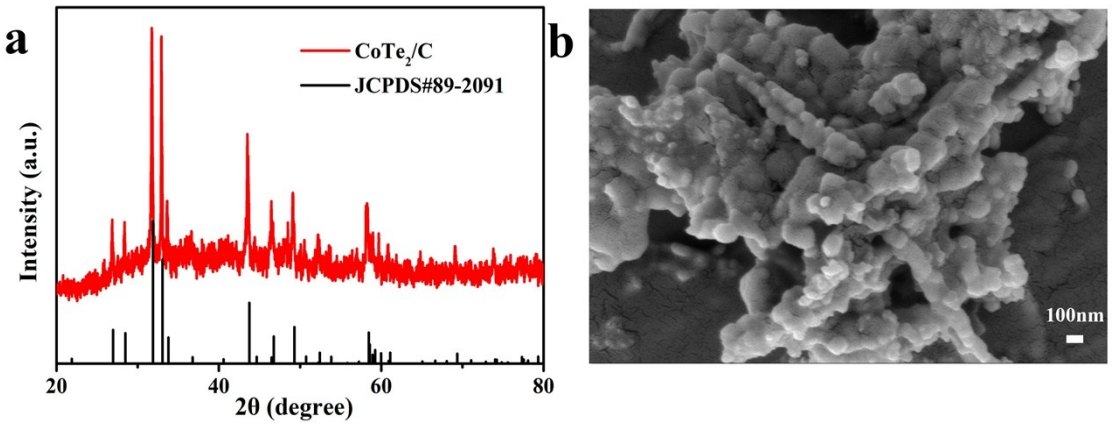

Fig. S2 (a) XRD pattern of $CoTe_2$/C nanoparticles. (b) SEM image of $CoTe_2$/C nanoparticles.

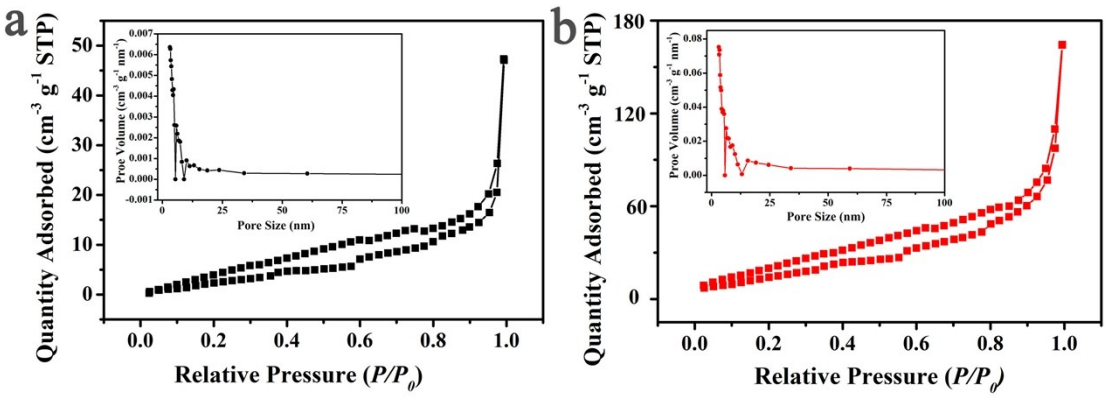

Fig. S3 N_2 adsorption isotherms of (a) pure $CoTe_2$/C nanoparticles and (b) P-$CoTe_2$/C nanoparticles, the inset images of (a) and (b) are the pore radius distribution of corresponding samples.

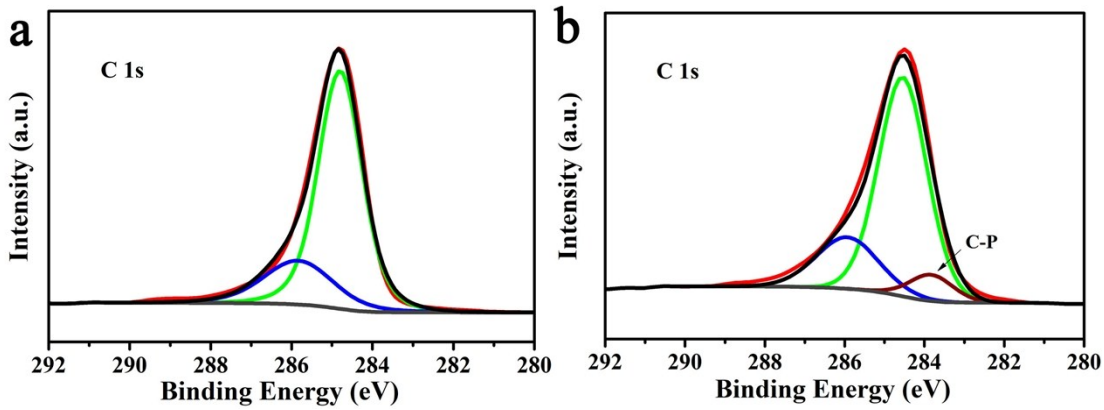

Fig. S4 (a) XPS spectrum of C 1s for the $CoTe_2$/C nanoparticles. (b) XPS spectrum of C 1s for the P-$CoTe_2$/C nanoparticles.

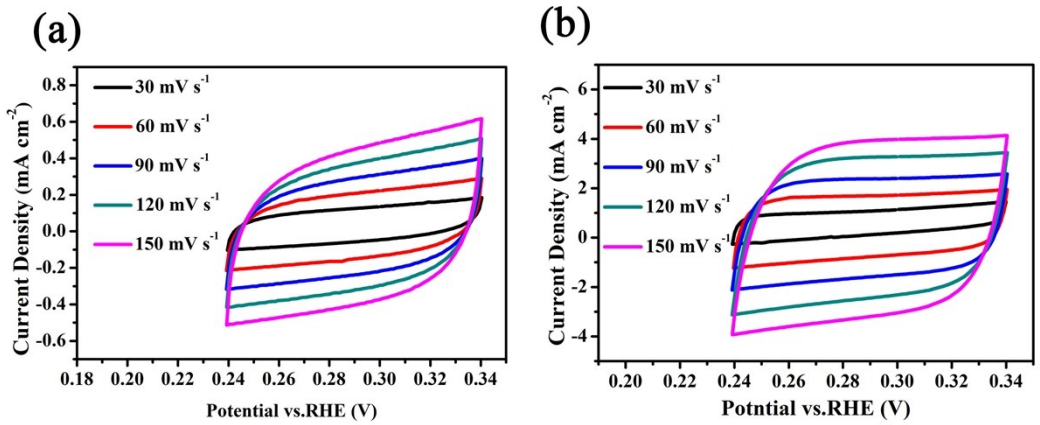

Fig. S5 The CV measurements of (a) $CoTe_2$/C and (b) P-$CoTe_2$/C in the potential region of 0.24-0.34 V (vs. RHE) in 0.5 M H_2SO_4.

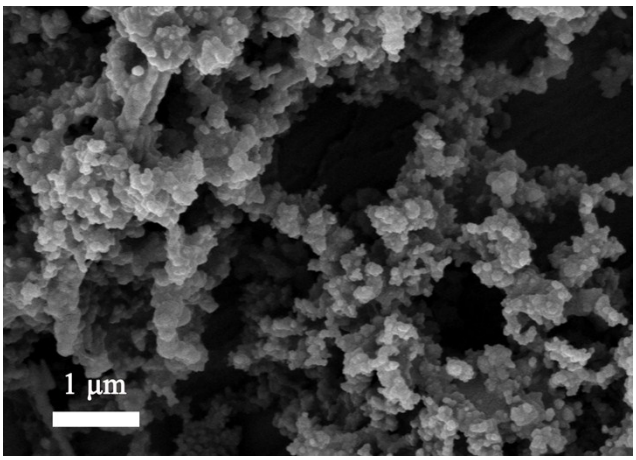

Fig. S6 SEM image of the P-$CoTe_2$/C electrode after 2000 CV cycles at scan rate of 100 mV s^{-1}.

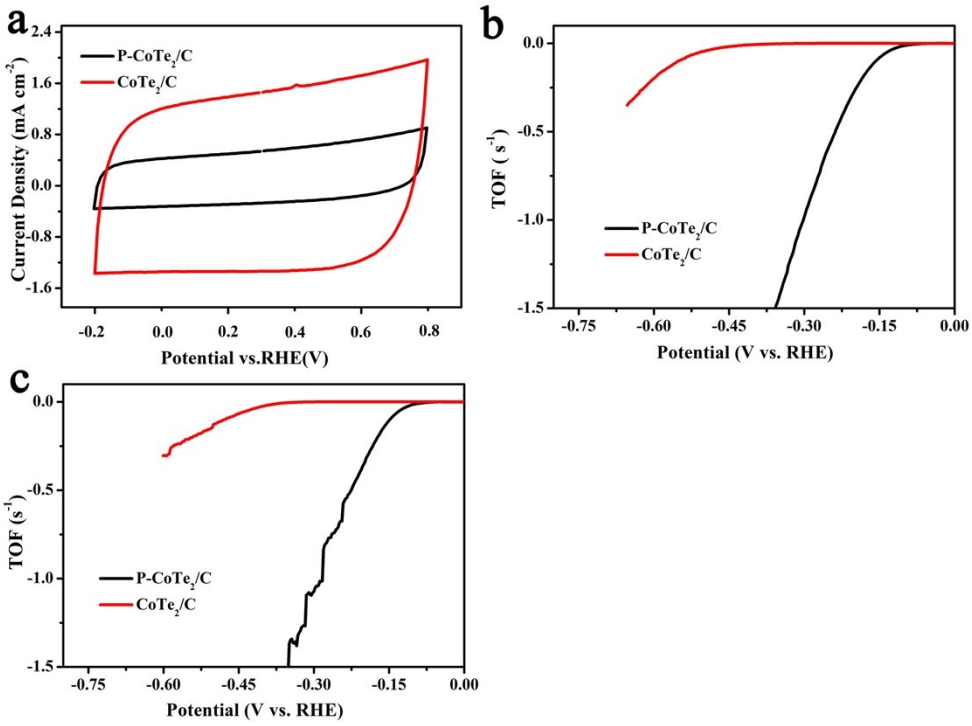

Fig. S7 (a) CV curves of the catalysts in 1.0 M PBS (pH=7) with scan rate of 50 $mV \cdot s^{-1}$. Calculated TOF of the catalysts for HER in (b) 0.5 M H_2SO_4 and (c) 1.0 M KOH.

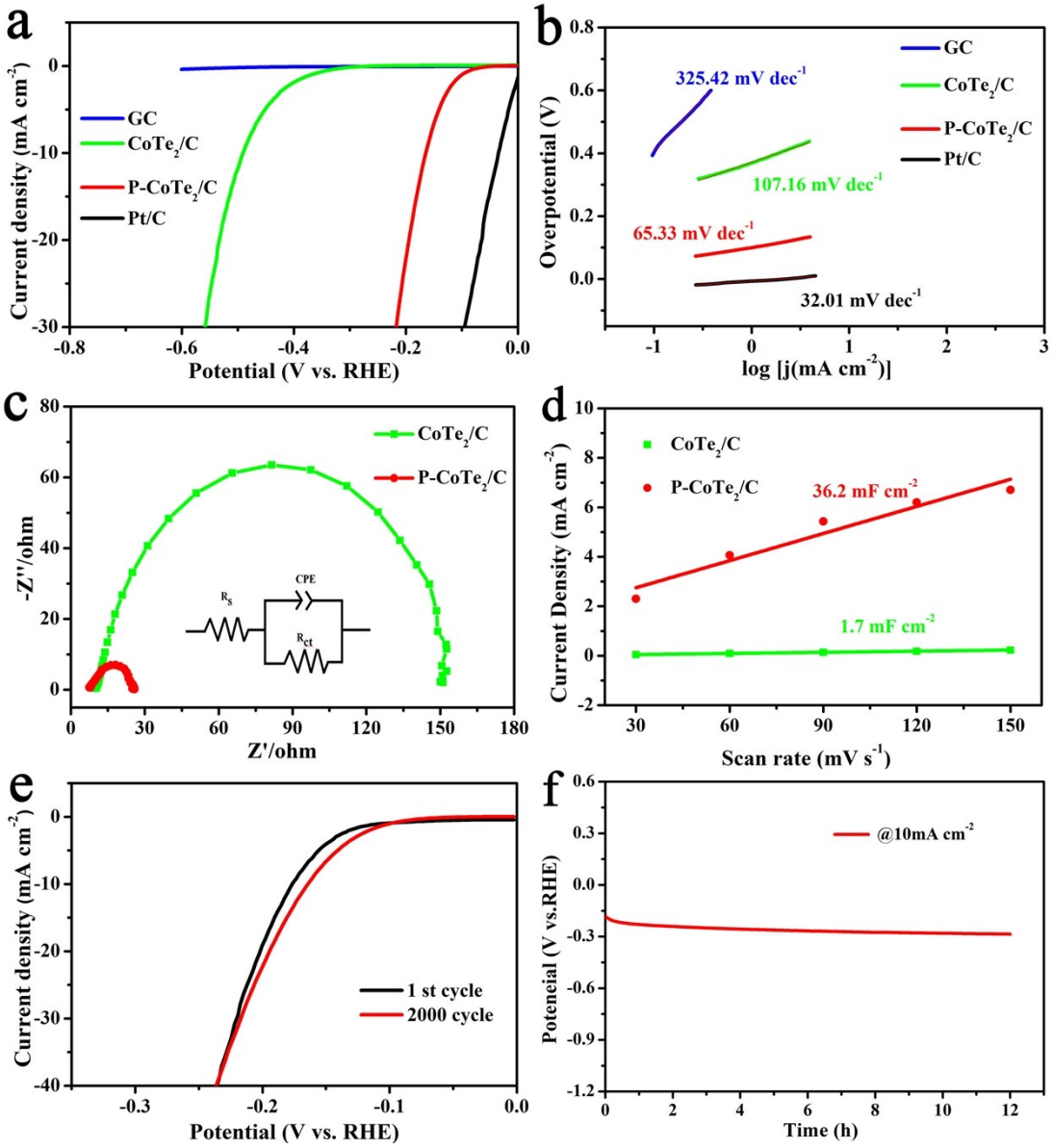

Fig. S8 Electrocatalytic HER measurements in 1 M KOH. (a) HER polarization curves of GC, $CoTe_2$/C nanoparticles, P-$CoTe_2$/C nanoparticles, and Pt/C at the scan rate of 5 mV s^{-1}. (b) The corresponding Tafel plots. (c) Nyquist plots of the $CoTe_2$/C nanoparticles and P-$CoTe_2$/C nanoparticles. (d) The difference of current density between the anodic and cathodic sweeps versus scan rate. (e) LSV curves of the P-$CoTe_2$/C nanoparticles before and after 2000 CV cycles. (f) chronopotentiometric curves at the current of 10 mA cm^{-2}.

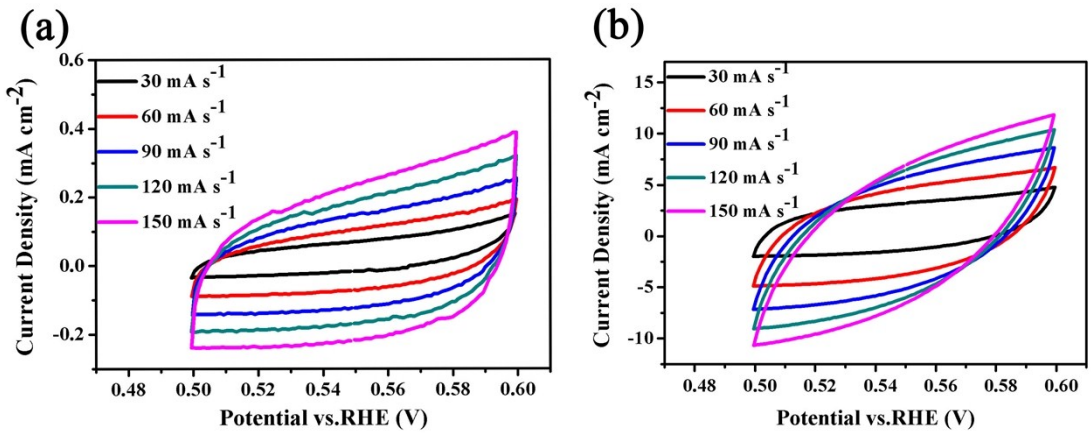

Fig. S9 The CV measurements of (a) $CoTe_2$/C and (b) P-$CoTe_2$/C in the potential region of 0.5-0.6 V (vs. RHE) in 1 M KOH.

As shown in Fig. S8a, when the current density was 10 mA cm^{-2}, the overpotential of the P-$CoTe_2$/C nanoparticles was 167 mV, and the overpotential of the $CoTe_2$/C nanoparticles was 483 mV. The doping of P also greatly improved the performance of $CoTe_2$/C nanoparticles in an alkaline environment. As shown in the Tafel plot in Fig. S8b, the Tafel values of P-$CoTe_2$/C nanoparticles and $CoTe_2$/C nanoparticles were 65.33 mV dec^{-1} and 107.1 mV dec^{-1}, respectively. This indicated that P-$CoTe_2$/C nanoparticles had a high HER activity. The illustration results in Fig. S8c showed that P-$CoTe_2$/C nanoparticles (28.7 Ω) exhibited a smaller charge transfer resistance than $CoTe_2$/C nanoparticles (148.1 Ω). It is shown that P-$CoTe_2$/C nanoparticles had higher charge transfer kinetics and lower contact resistances than $CoTe_2$/C nanoparticles. The double-layer capacitance (C_{dl}) was tested under alkaline conditions. The CV tests were measured in the potential range of 0.5 to 0.6 V (vs RHE) at the scan rate of 30, 60, 90, 120, and 150 mV s^{-1}(Fig. S9). As shown in Fig. S8d, the C_{dl} value of P-$CoTe_2$/C nanoparticles was calculated as 36.2 mF cm^{-2}, much higher than that of $CoTe_2$/C nanoparticles (1.7 mF cm^{-2}). As shown in Fig. S8e, after 2000 consecutive CV cyclic voltammetry scans, the HER catalytic activity was only weakly attenuated, indicating superior stability of the P-$CoTe_2$/C nanoparticles. At the same time, the P-$CoTe_2$/C nanoparticles were tested for long-term stability in a 1 M KOH solution at a constant current density of 10 mA cm^{-2}. As shown in Fig. S8f, the voltage of P-$CoTe_2$/C nanoparticles increased only slightly after 12 h, further indicating that P-$CoTe_2$/C nanoparticles had an excellent catalytic stability of HER.

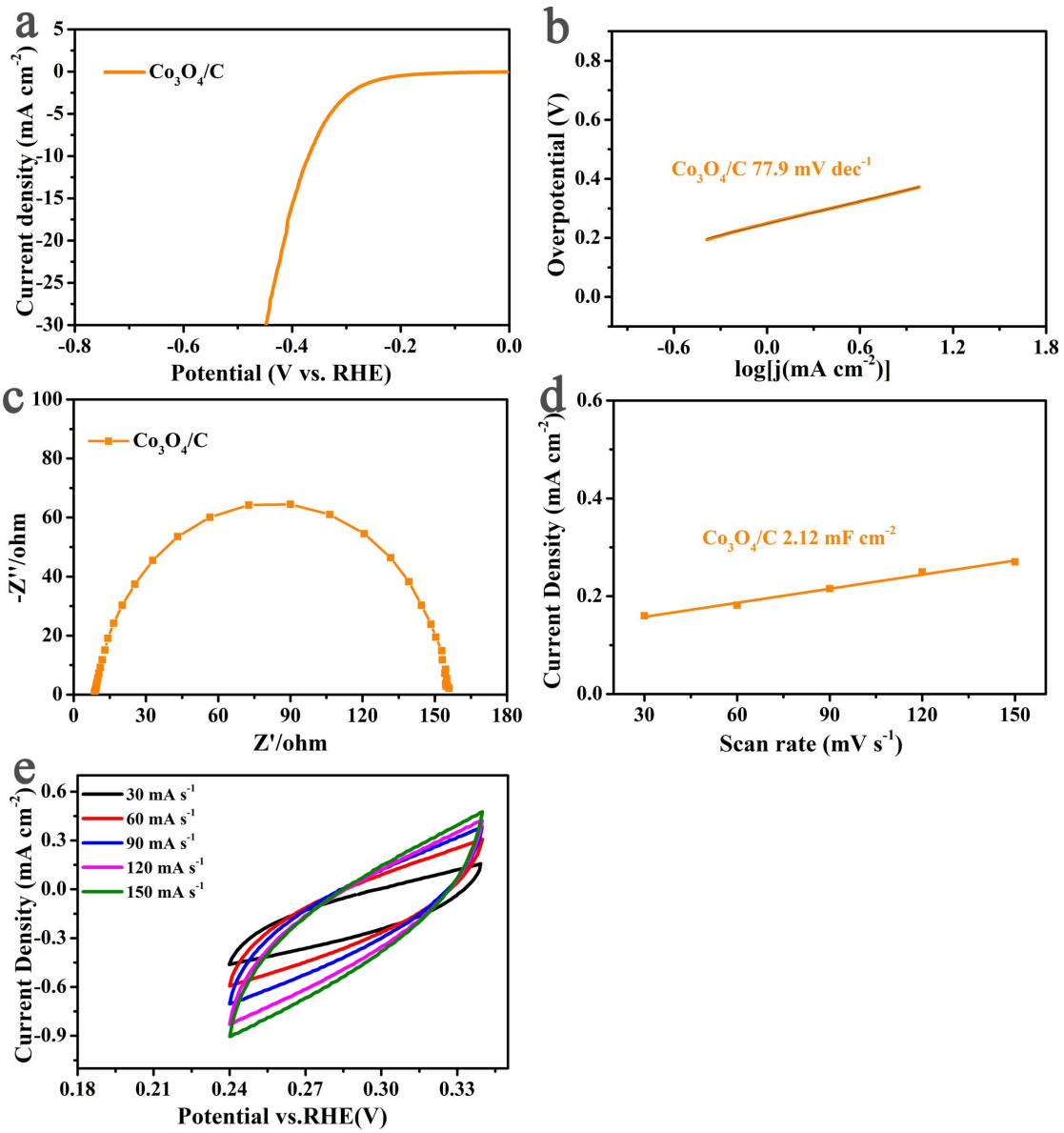

Fig. S10 Electrocatalytic HER measurements in 0.5 M H_2SO_4. (a) HER polarization curves of Co_3O_2/C nanosheets at the scan rate of 5 mV s^{-1}. (b) The corresponding Tafel plots. (c) Nyquist plots of the Co_3O_2/C nanosheets. (d) The difference of current density between the anodic and cathodic sweeps versus scan rate. (e) The CV measurements of Co_3O_2/C nanosheets in the potential region of 0.24-0.34 V (vs. RHE) in 0.5 M H_2SO_4.

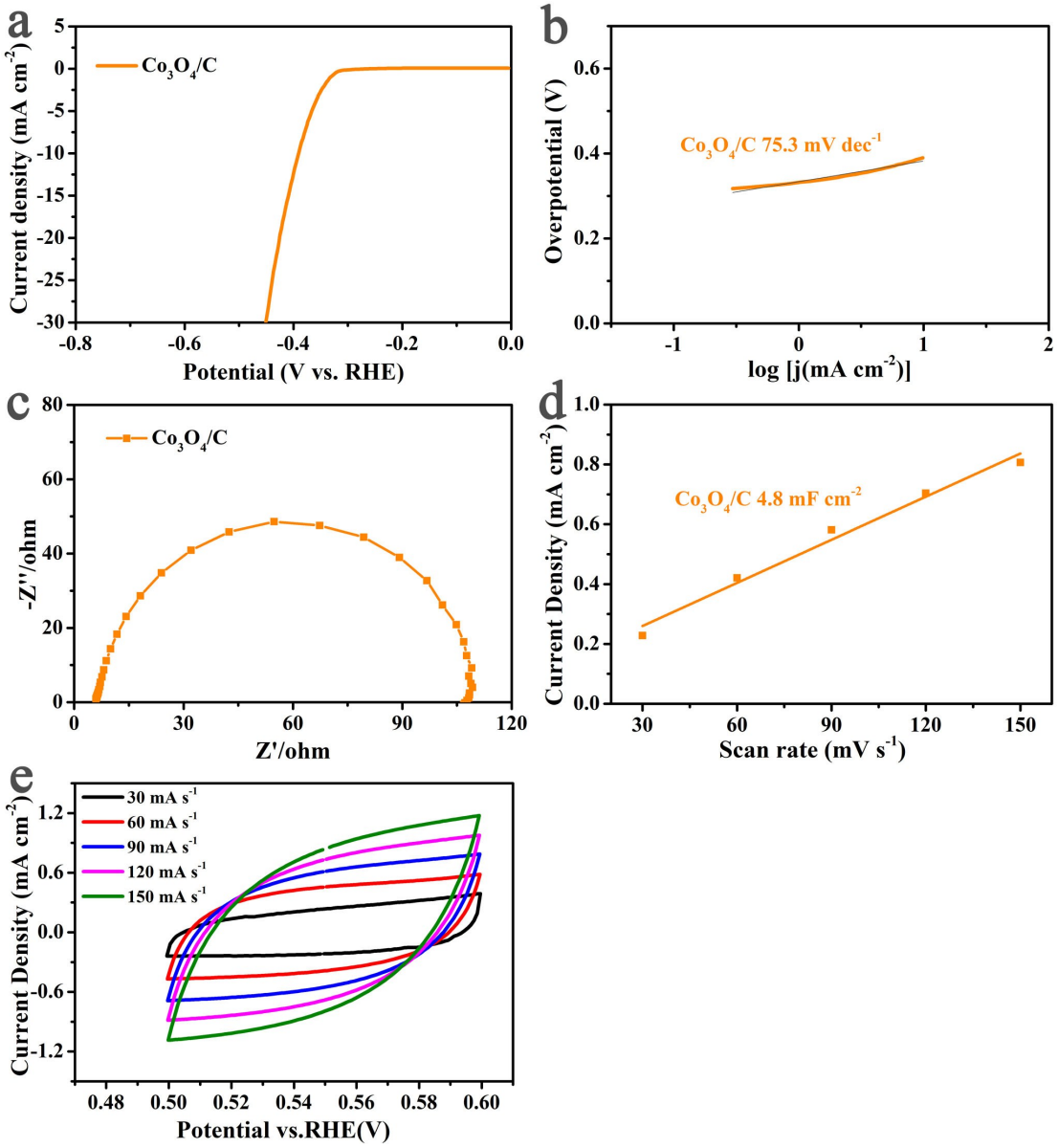

Fig. S11 Electrocatalytic HER measurements in 1 M KOH. (a) HER polarization curves of Co_3O_2/C nanosheets at the scan rate of 5 mV s^{-1}. (b) The corresponding Tafel plots. (c) Nyquist plots of the Co_3O_2/C nanosheets. (d) The difference of current density between the anodic and cathodic sweeps versus scan rate. (e) The CV measurements of Co_3O_2/C nanosheets in the potential region of 0.5-0.6 V (vs. RHE) in 1 M KOH.

Table. S1 Comparison of HER performance for as-synthesized catalysts with other non-noble HER catalyst.

Catalyst	Electrolyte	η_{10}（mV）	Tafel slop (mV dec^{-1})	Reference
P-$CoTe_2$/C	1M KOH	167	65.33	This work
P-$CoTe_2$/C	0.5 M H_2SO_4	159	64.62	This work
$Co_{1.11}Te_2$/C	1M KOH	178	77.3	[5]
$CoTe_2$/C	1M KOH	295	97.8	[5]
CoTe/C	1M KOH	397	115.1	[5]
$CoTe_2$@NCNTFs	1M KOH	234	77.6	[6]
$CoTe_2$	0.5M H_2SO_4	580	51	[7]
$NiTe_2$	0.5M H_2SO_4	560	44	[7]
CoTe NSs/$CoTe_2$ NTs	0.5M H_2SO_4	172	57.1	[8]
CoTeNR/NF	1M KOH	202	115	[9]
NiTeNR/NF	1M KOH	248	185	[9]
$MoTe_2$ Ns	0.5M H_2SO_4	309	119	[10]
$CoTe_2$@NF	0.5M H_2SO_4	111	79	[11]
Ni-Fe-MoN NTs	1M KOH	55	109	[12]
CoPh/NG	1M KOH	83	57	[13]

Reference

1. G. Kresse and J. Furthmuller, *Phys Rev B Condens Matter*, 1996, **54**, 11169-11186.
2. G. Kresse and D. Joubert, *Phys. Rev. B*, 1999, **59**, 1758.
3. D. Y. Wang, M. Gong, H. L. Chou, C. J. Pan, H. A. Chen, Y. Wu, M. C. Lin, M. Guan, J. Yang, C. W. Chen, Y. L. Wang, B. J. Hwang, C. C. Chen and H. Dai, *Journal of the American Chemical Society* 2015, **137**, 1587-1592.
4. B. Chen, I. A. Meinertzhagen and S. R. Shaw, *J Comp Physiol A*, 1999, **185**, 393-404.
5. H. Wang, Y. Wang, L. Tan, L. Fang, X. Yang, Z. Huang, J. Li, H. Zhang and Y. Wang, *Applied Catalysis B: Environmental* 2019, **244**, 568-575.
6. X. Wang, X. Huang, W. Gao, Y. Tang, P. Jiang, K. Lan, R. Yang, B. Wang and R. Li, *Journal of Materials Chemistry A* 2018, **6**, 3684-3691.
7. X. Chia, Z. Sofer, J. Luxa and M. Pumera, *Chemistry* 2017, **23**, 11719-11726.
8. K. Wang, Z. Ye, C. Liu, D. Xi, C. Zhou, Z. Shi, H. Xia, G. Liu and G. Qiao, *ACS applied materials & interfaces* 2016, **8**, 2910-2916.
9. L. Yang, H. Xu, H. Liu, D. Cheng and D. Cao, *Small Methods* 2019, **3**, 1900113.
10. H. Qiao, Z. Huang, S. Liu, Y. Liu, J. Li and X. Qi, *Ceramics International* 2018, DOI: 10.1016/j.ceramint.2018.08.166.
11. Y. Yin, J. Xu, W. Guo, Z. Wang, X. Du, C. Chen, Z. Zheng, D. Liu, D. Qu, Z. Xie, H. Tang and J. Li, *Electrochimica Acta* 2019, **307**, 451-458.
12. C. Zhu, Z. Yin, W. Lai, Y. Sun, L. Liu, X. Zhang, Y. Chen and S.-L. Chou, *Advanced Energy Materials* 2018, **8**, 1802327.
13. X. Yu, S. Zhang, C. Li, C. Zhu, Y. Chen, P. Gao, L. Qi and X. Zhang, *Nanoscale* 2016, **8**, 10902-10907.